

Paris le 14/02/75

Study of the K^+p -Interactions at

250 - 300 GeV/c

by means of a Rapid Cycling Bubble

Chamber set-up

A. Stergiou, Y. Goldschmidt-Clermont

CERN

E. Hafen, I. Pless, R. Yamamoto

M.I.T.

W. Kittel^(*), W. Metzger, C. Pols,
J. Schotanus and R. Van de Walle

Nijmegen

Abstract

We propose a study of K^+p -interactions at 250-300 GeV/c in a hybrid rapid cycling bubble chamber set-up equipped with downstream equipment for momentum measurement and particle identification. In this energy region the K^+p -reactions are in the ISR-regime of rising cross-sections; using incident K^+ 's will avoid the symmetry of the pp -reactions and in addition have the advantage of a beam particle with a traceable identity in the final state. The required interactions will be obtained by tagging and flash-triggering in an enriched K^+ -beam. The main physics aims are topological cross-sections, single- and two-particle inclusive channels, semi-inclusive channels, leading particle peaks, double diffraction dissociation and central particle emission. We are requesting an exposure of 10 events/ μb or about 200K pix. in approx. 35 days running time.

CERN LIBRARIES, GENEVA

(*)Contact person: E.W. Kittel



CM-P00059054

1. INTRODUCTION

The total cross-section for K^+p -reactions increases by more than 10% from 30 to 300 GeV/c incoming lab. momentum. To some extent K^+p -reactions at FNAL and SPS-energies can therefore be expected to resemble pp-reactions at ISR-energies.

To investigate to what extent this similarity indeed exists is the first main aim of the experiment we propose; it would be primarily examined in inclusive and/or low-multiplicity exclusive channels. In as far as such a similarity would indeed be observed, an advantage of the K-beam would be that it avoids the symmetry of the pp-reactions. Over $\pi^\pm p$ reactions, $K^\pm p$ -interactions have the added advantage that the identity of the beam particle can be traced in the final state.

The second main aim of our experiment is the study of topological cross-sections, central emission, resonance production and double diffraction dissociation in medium and high multiplicity 4C exclusive channels.

We propose an exposure of approx. 10 events/ μb with a K^+ -beam between 250 and 300 GeV/c in a rapid-cycling bubble chamber coupled to a downstream device allowing secondary particle identification. A set-up as discussed and described in ref. [1] would meet our requirements. The capabilities of such RCBC set-up in terms of resolution, accuracy, completeness and versatility have been discussed at length in the above reference, and more recently, repeated and expanded in a proposal to the SPSC by a CERN-Orsay-Oxford-Rutgers-Stockholm collaboration [2]. This discussion will not be repeated here. For completeness we show in table 1 the main parameters of the above mentioned proposal and in Fig. 1 the suggested lay-out. We are still examining the need for an extra downstream Cerenkov to cover the region above the ISIS-cut off of 50-60 GeV/c (containing approx. $\leq 10\%$ of all secondaries).

2. PHYSICS MOTIVATIONS

The program sketched in the introduction will be executed in several steps. Among the most important of these are:

(a) Study of Topological Cross Sections;

Topological cross sections are predicted for 75, 150 and 300 GeV/c incoming lab. momentum in fig. 2. These cross section values have been calculated from the K^+p data at 32 GeV/c [3] under the assumption of

1. a logarithmic increase of the total cross section [4] and average charge multiplicity
2. a KNO scaling law.

Table 2 gives - per prong number - the estimated number of events for a 10 events/ μb exposure at 250 GeV/c.

These predictions are rough and can be used only for a provisional planning of the experiment. How the energy dependence of particularly the low multiplicity reactions (diffraction dissociation) actually contributes to the total cross section will have to be answered from the first experimental results themselves. The multiplicity distribution and its statistical moments can be obtained essentially already from the scanning of photographs from the bare vertex detector.

(b) Elastic Cross Section at low t .

Of immediate interest in connection with the increasing total cross section is the elastic cross section. One usually distinguishes between three regions.

- a) very small t ($|t| \leq 0.05 \text{ GeV}^2$) for the estimation of the real to imaginary part ratio ρ . The value of ρ can be of interest for the prediction of the further increase of σ ,
- b) small t ($0.05 \lesssim |t| \lesssim 0.30 \text{ GeV}^2$) for the estimation of the slope or the slopes of the forward peak and their shrinkage,
- c) large t ($|t| \gtrsim 0.3 \text{ GeV}^2$) for the search of diffraction minima.

While this is a-priory a typical counter experiment, high quality data have been obtained in particular for point (a) as a "by-product" of bubble chamber K^+p experiments at 4.2, 10 and 14.3 GeV/c [5].

The downstream MPWC-system will provide a sensitive technique for separating elastic from inelastic events in the 2-prong sample [6]. The measurement of the proton momentum (up to a few MeV/c) from the range in hydrogen then results in a high measurement precision for the low $|t|$ elastic events, independent of the incident energy.

c. Leading particle peaks at low t : Diffractive Mechanisms

a) a leading K^+ may be used to separate proton dissociation,

b) a leading backward proton may be used to separate K^+ dissociation.

One dimensional Feynman x - or missing mass distributions contain large overlap of diffraction dissociation and other mechanisms. This overlap makes the estimation of the diffractive cross section as well as a further study of diffraction dissociation a difficult task. We therefore plan an attempt of separation of diffraction dissociation in two- and more dimensional inclusive distribution. Besides conventional separation methods we intend to make extensive use of newly developing "cluster" searching techniques [7]. We therefore need to know the momenta of leading and as far as possible also the non-leading particles. After and only after clean separation of diffraction dissociation, can factorization properties be meaningfully tested [6]:

$$\frac{\sigma_{K^+p}(\text{elastic})}{\sigma_{pp}(\text{elastic})} = \frac{\sigma_{K^+p}(\text{leading } K^+p)}{\sigma_{pp}(\text{leading } p)}$$

$$\frac{\sigma_{K^+p}(\text{elastic})}{\sigma_{\pi^\pm p}(\text{elastic})} = \frac{\sigma_{K^+p}(\text{leading } K^+)}{\sigma_{\pi^\pm p}(\text{leading } \pi^\pm)}$$

We would like to study whether there is more than one diffraction component. It should be stressed that a study of diffractive behaviour (or Pomeron exchange) in an incident K^+ beam has the advantage over K^- , that no interference with non-Pomeron $I=0$ exchange processes (f , ω -exchange) can occur. (*)

(*) The f, ω -trajectories contribute to K^+ and K^- processes in the form $f + \omega$ (purely real) and $f - \omega$ (purely imaginary) resp.

d) Correlations in Semi-inclusive Channels

The topological semi-inclusive distributions mentioned under a) will also be used to examine correlations in momentum, azimuth and hemisphere both between like and unlike final state particles. Again we will make thereby use of the newly developed "clusters" searching techniques referred to under c)

e) Resonance Production

. Leading Resonance Production

The mechanism of resonance production at high energies is of great importance. In particular, K_{890}^* production is allowed to proceed by pomeron exchange from the quark model [8], but forbidden by the Gribov-Morrison rule [9]. Should K_{890}^* production be allowed by pomeron exchange, we could expect a leading K_{890}^* peak, similar to the K^+ peak. The partial wave analysis of 3π system [10] grants a rather flat energy dependence for the $J^P=2^+$ component. If a similar behaviour exists in the $K\pi\pi$ system, one can expect a nonzero amount of K_{1420}^* production at high energies, as well.

While "diffractive" K^* production is an open question, diffractive N^* production is present. The question there is the exact mechanism [11]. We believe that as much information as possible has to be collected. K^+p reactions can contribute to the study of factorization properties.

Other questions related to diffractive excitation which will be studied are:

. The shape (width) and cross-sections for both the Q and the L enhancements (the exposure should yield some 5000 4C events of the type $K^+p \rightarrow K^+p\pi^+\pi^-$)

. The diffractive dissociation of $K^+ \rightarrow p\bar{\Lambda}$.

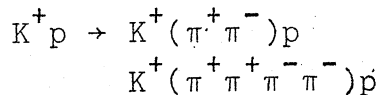
. Cascade Production

The main part of resonance production will probably proceed via cascade decay of peripherally or centrally produced clusters. If we can trace the K^+ (or K^0) in the final state we have the advantage over incoming pions of less identical particles. As a result of baryon-cascades we expect copious production of the $\Delta^{++}(1236)$ in the backward c.m. hemisphere [12].

f) Central Emission; Central Clusters

The mechanisms usually summarized as 'central emission' give the largest contribution to the total cross section. They involve high multiplicity reactions which are difficult to study. Therefore relatively little is known here.

The simplest problem is that of "central emission" of a neutral pion pair in a four-body final state via double pomeron exchange. It is not yet clear whether this mechanism exists. One can expect to get useful information from the (asymmetric) $K^\pm p$ four body final states (4C fit):

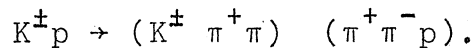


g) Double Diffraction Dissociation

Double Diffraction Dissociation is expected to contribute to the total cross section with a sizeable amount (0.5 - 1.0 mb estimated from factorization). Nevertheless little is known about it so far.

Monte Carlo calculations [13] for the SFM show that diffraction dissociation almost completely overlaps with central emission even on two-dimensional inclusive x -plots.

We expect that diffraction dissociation can be studied better in medium-multiplicity exclusive 4C fits like



for which we expect a 10 - 20 μ b cross section.

At high energies one can expect to separate it from single diffraction dissociation and central emission with multidimensional cluster searching techniques as mentioned in sect. C. From factorization we expect diffractive and double diffractive components in the inelastic topological cross sections satisfying the relation [6]:

$$\sigma_{in}^n = \sigma_{lK^+}^n + \sigma_{lp}^n + \frac{1}{\sigma_{el}} \sum_{j=0}^{n-2} \sigma_{lK^+}^{n-2j} \sigma_{lp}^{2j+2}$$

with

- σ_{in}^n the topological cross section for producing n charged particles
- σ_{el} the elastic $K^+ p$ cross-section
- $\sigma_{lK^+}^i, \sigma_{lp}^i$ the leading K^+ and the leading proton cross section for the i charged prong multiplicity.

3. BEAM

A major problem of the experiment is the K^+ -beam. For the energies considered here, separated beams are out of question. The required K^+ -beam will have to be obtained by enriching and tagging. The picture taking efficiency will be increased by flashtriggering [2].

Assuming a RCBC with a 30Hz cycling rate, a fiducial volume of $\sim 50\text{cm}^3$ and a maximum of 10 beam particles/picture, an enriched beam will become useful for bubble chamber physics where the wanted particles are of the order of 10% of the total particle flux. With one K^+ per bubble-chamber expansion one then collects approx. one useful event per SPS-cycle or approx. 6000 events/day.

Neal has suggested and discussed enrichment schemes for use with the FNAL bubble chambers [14]. For a K^+ -beam only the filterscheme seems compatible with the SPS-north area target lay-out and slow spill. Possible filter schemes have been considered by N. Doble and B. Powell [15]; the presently preferred solution is to use beam line H2 from target T2 and locate a filter at the entrance of the tunnel which links the target enclosure to EHN1., immediately after the vertical bend TT81 leading into the tunnel. The filter would be situated at a focus to minimize the effect of the filter on the transmitted component.

The beam-line T2 has a length of $\sim 500\text{m}$, and a $\Delta\Omega \cdot \Delta p/p$ of $2\mu\text{sr} \times 2\%$; it can carry beams up to 340 GeV/c. The second vertical bend at the entrance of EHN 1 forms a spectrometer allowing particle momenta determinations up to $\Delta p/p \approx 0.2\%$. A Cerenkov-counter (CEDAR) allowing identification of particles up to 340 GeV/c completes the beam.

The crucial question now is whether this set-up will produce an acceptable K^+ -flux. The following factors are relevant for the answer(*)

(*) For the sake of concreteness we will concentrate our discussion on 250 GeV/c secondary momenta; for reasons explained later we will actually try to perform the experiment as close to 300 GeV/c as the K^+ beam-intensity will allow.

(a) the p/ π^+ /K $^+$ proportions at production

Assuming an incident proton momentum of 400 GeV/c, a flux of $3 \cdot 10^{12}$ incident protons ($\sim 10^{12}$ interacting protons) we find the following secondary particle fluxes at 250 GeV/c [15]

$$\begin{aligned} p &\sim 8.0 \cdot 10^8 \\ \pi^+ &\sim 6.0 \cdot 10^7 \\ K^+ &\sim 1.2 \cdot 10^7 \end{aligned}$$

or the ratio's : $p/\pi^+ \simeq 13$; $\pi^+/K^+ \simeq 5$

The above numbers correspond with the minimum attainable production angle (~ 2 mrad). In general the π^+/K^+ ratio can be reduced by going to larger production angles; for secondary momenta > 200 GeV/c derived from a 400 GeV/c incident beam however, the effect has disappeared.

(b) the enrichment produced by the filter

The muon component is the main limitation on the usable filter thickness; the main muon background comes from the particles decaying before the filter within the phase-space of the transmitted beam component. Preliminary calculations indicate that a filter reducing the p-component by a factor 1000 is approx. the maximum filter thickness that one can accept. For such an absorption factor the μ -background in the beam entering the bubble chamber will amount to approx. 10% [16]. A drop in the proton-flux by a factor 1000 requires a filter with approx. thickness of 7 absorption lengths; this corresponds to approx. 5.2 meter of water (or polyethylene) or 2.5 meter of beryllium. Using a filter of this thickness and the measured or extrapolated pp , π^+p and K^+p cross sections at 250 GeV/c [4] one derives the following (theoretical) flux-reduction factors:

$$\begin{aligned} p &\sim 1/1000 \\ \pi^+ &\sim 1/73 \\ K^+ &\sim 1/40 \end{aligned}$$

or, the improvement factors:

$$\begin{aligned} &\times 14 \quad \text{for the } \pi^+/p\text{-ratio} \\ &\times 1.85 \quad \text{for the } K^+/\pi^+\text{-ratio} \end{aligned}$$

Tests on π^+/p ratio's have been made by Neal at NAL using a 200 GeV/c positive beam and a filter corresponding to 5.4 ab-

sorption lengths; an improvement of x7 was obtained. A calculation as above predicts a factor 8. A preliminary K^+/π^+ -ratio test using an 60 cm polyethylene target yielded the result $1.08 \pm .03$; theoretically one predicts a factor 1.08. Although there are still uncertainties, the preliminary conclusion seems to be that the filters roughly perform as expected.

It has furthermore been checked that the divergence introduced by a filter as proposed here, is acceptable for the CEDAR-Cerenkov counter used for tagging [17].

(c) the decay losses

For a beam length of 500 meter and particles of 250 GeV/c momentum the decay-losses are 4% (π) and 25% (K) resp.

Combining the above numbers we arrive at the following fluxes at the entrance of the RCBC for 250 GeV/c secondary particles and 10^{12} interacting protons:

p	$\sim 8 \cdot 10^5$
π^+	$\sim 8 \cdot 10^5$
K^+	$\sim 2 \cdot 10^5$
Total (per spill)	$18 \cdot 10^5$

These numbers indicate that a K^+ -density of 10% can be reached.

To obtain an intensity of 10 beam particles per picture i.e. 10 particles per 0.5 msec. (=sensitive time of the bubble chamber) during a slow spill of 700 msec. we actually don't need more than $14 \cdot 10^3$ particles per spill. This intensity will lead to a beam (per picture) consisting of: 4/5 p; 4/5 π^+ ; 1 K^+ and (for a fiducial volume of 50cm) to 0.7 K^+ -interactions per 20 expansions or per SPS-cycle. The expansion containing the K^+ -interaction will be selected by tagging and an interaction trigger. In approx. 50% of the cases the picture taken will contain a second (p or π) interaction; in 10% even two additional interactions.

4. USE OF A RCBC AS AN OPTICAL VERTEX DETECTOR

The power of an optical vertex detector for high multiplicity final states is by now well known. It is ideally matched to the kinematics of the target fragmentation and interactions (or decays) close to the production vertex. Coupled to a downstream spectrometer and to devices allowing identification of secondary particles it becomes a powerful tool to study leading particle processes as well as medium and high multiplicity exclusive channels. The availability of all these features, without complex pattern recognition problems, is of crucial importance for the experimental program which we propose.

It is worthwhile to consider the use of a streamer chamber instead of a RCBC. A streamer chamber can handle up to 10^6 particles per sec. or $7 \cdot 10^5$ particles per spill (a factor 50 with respect to the RCBC). The trigger rate however is limited by film moving to ~ 15 per second. In addition, to minimize systematic errors from secondary interactions in the target, one has to use a substantially smaller target length than 50 cm. For a secondary interaction contamination in 6 prongs of $\lesssim 1\%$ a target of not more than 4 cm. has to be used. Assuming that we are interested in collecting the same data, i.e. that we stay with the trigger cross sections implied by the preceding physics motivations, the data-taking rate advantage of the streamer chamber over the RCBC is only a factor $\lesssim 5$. This advantage is in our opinion largely offset by the following features of the RCBC

- (a) better point-precision (50μ vs. 300μ)
- (b) better resolution (200μ vs. 2 to 6 mm.)
- (c) greater isotropy
- (d) sensitive H_2 -target with smaller recoil $|t \min|$ detection (0.01 GeV^2 vs. 0.05 GeV^2)
- (e) better identification for low momentum ($\leq 1.5 \text{ GeV}/c$) particles.

Recent hybrid experiments at F.N.A.L. have shown that especially feature (a) is of great importance in making optimal use of downstream spectrometers [6].

5. EXPOSURE AND ANALYSIS

We request an exposure of 200K pictures or approx. 35 running days. This will yield a sample of 10 events/ μb . The amount of pictures requested is primarily determined by the statistics needed for the study of the low cross section 4C-channels.

The participating groups have at present the measuring capacity to handle the requested number of events in approx. one year.

The CERN and Nijmegen groups have submitted proposals for a BEBC 70 GeV/c K^+p experiment. The M.I.T. and Nijmegen groups intend to collaborate in an exposure of the 30" HBC at FNAL to a 150 GeV/c K^+p -beam. An exposure in the region of 250-300 GeV/c incident momentum would permit interesting energy-dependent analyses; where the above calculations indicate that (intensity-wise) the experiment will be possible around 250 GeV/c incident momentum, we intend to select the final momentum as close to 300 GeV/c as the K^+ -intensity will allow.

Acknowledgements

We would like to thank H. Atherton, N. Doble, W. Neale and B. Powell for useful discussions.

- [1] W. Allison et al. "The advantages of a RCBC at SPS-energies" CERN/SPSC/74-45/T14 and Add. 1.
- [2] Proposal to SPSC - "Study of multi-hadron events involving identified particles in high energy interactions" CERN-Orsay-Oxford-Rutgers-Stockholm. CERN/SPSC/75-15/P42.
- [3] G.A. Akopdjanov et al., Nucl. Phys. B75 (1974) 401 .
- [4] BNL - Fermilab-Rockefeller Collaboration, XVII Int. Conf. on High Energy Physics, London 1974.
- [5] U. Amaldi, IInd. Int. Conf. on Elementary Particles, Aix-en-Provence 1973, page C1-252.
- [6] D.G. Fong et al., Phys. Letters 53B (1974) 290.
- [7] G. Friedman "Data Analysis Techniques for High Energy Particle Physics" Proc. 1974 CERN School of Computing, CERN 74-23
W. Kittel "Treating Multiparticle Processes". Proc. Symposium on Antinucleon-Nucleon Interactions" Liblice-Prague 1974, CERN 74-18.
- [8] P.G.O. Freund, H.F. Jones and R.J. Rivers, "Dynamics versus selection rules in diffraction dissociation", Imperial College preprint ICTP/70/35.
- [9] V.N. Gribov, Yadernaya Fiz./U.S.S.R./5 (1967) 197,
D.R.O. Morrison, Phys. Rev. 1965 (1968) 1699.
- [10] G. Ascoli, "Results on $\pi^{\pm}p \rightarrow \pi^{\pm}\pi^{+}\pi^{-}p$ ", XVII Int. Conf. on High Energy Physics, London 1974.
- [11] G. Berlad et al. Phys. Letters 51B (1974) 187,
E. Nagy et al., "Experimental Results on Inelastic Diffraction Scattering in Proton-Proton Collisions at the ISR".
- [12] F.T. Dao et al., Phys. Rev. Lett. 30 (1973) 34.
- [13] W. Kittel, W. Schwille and H. Wahl. Internal SFM Group Report, Jan. 1974.
- [14] W.W. Neale "Enriched Particle Beams for the bubble chambers at FNAL" FNAL 259.

[15] N. Doble and B. Powell - Private communication and ref. [2]

[16] B. Powell - private communication.

[17] C. Bovet - private communication.

Table 1.

Main Parameters for RCBC set-up

1. RCBC

Diameter	80 cm
Depth	40 cm
Fiducial length	50 cm
Precision	50 μ
Cycling rate	15 - 30 H _z

2. Vertex- Magnet (M1)

Type	superconducting
Field	30 KG
Coil-diameter	210 cm
Coil-gap	90 cm
Acceptance: horiz.	$\pm 15^\circ$
vert.	$\pm 30^\circ$

3. Cerenkov-hodoscope (C1)

Radiator	Freon 12 (3.3 atm.)
Height	3.8 m
Diameter	1.6 m
π -threshold	1.6 GeV/c
K-threshold	5.6 GeV/c

4. ISIS

Gas:	A + CO ₂ (20%)
Dimensions (L x H x D)	(5 x 4 x 2)m ³
Separation	
π -K	3 - 50 GeV/c
π -p	3 - 100 GeV/c
K-p	5 - 80 GeV/c

5. Spectrometer Magnet (M₂)

Bending power	4 T m,
Aperture	(40 x 100)cm ²
$\Delta p/p$	$\lesssim 1\%$
Range	50 - 200 GeV/c
Acceptance (at 50 GeV/c)	80%

Table 2.

Estimated number of events for a 10 events/ μb exposure
at 250 GeV/c (200K pix; 1 K^+ /picture; 50 cm fiducial volume)

<u>No. of prongs</u>	<u>Number of events</u>
2 (el)	35.000
2 (inel.)	9.000
4	27.000
6	39.000
8	37.000
10	30.000
12	14.000
14	7.500
16	3.000
18	1.300
20	200
Total	203.000

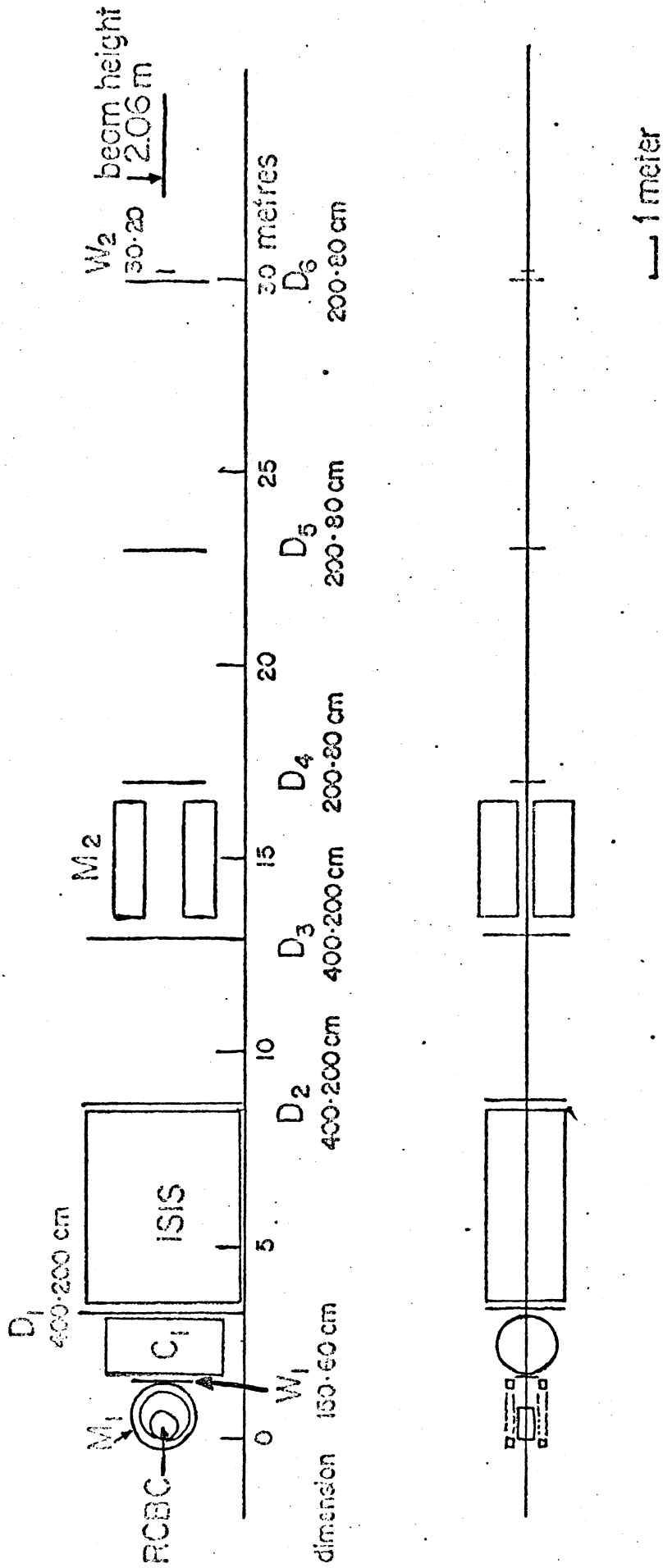


Fig. 1.

FIG. 2

